

文章编号: 1006-9941(2007)01-0023-06

Investigation of Three-point Detonation Mechanism and Formation of Tails of EFP

LI Cheng-bing¹, SHEN Zhao-wu¹, PEI Ming-jing²

(1. Department of Modern Mechanics, University of Science and Technology of China, Hefei 230026, China;

2. Northwest Poly University, Xi'an 710072, China)

Abstract: The detonation wave theory was applied to analyze the interacting process of detonation waves after the shaped charge was initiated with three initiation points. And the forming process and mechanism of the hyper pressure on the symmetrical plane were obtained. The energy sources forming the EFP tails were found. The software of LS-DYNA was simulated the impacting process of detonation waves, the formation of hyper-pressure, and the deforming process of the liner. Results of simulations show the liner overturns and deforms under the action of the nonuniform loads of explosive and three pressure marks on the surface of liner are forged by hyper pressure. The displacement-time curves indicate the formation of the EFP tails is attributed to the different displacements of elements of the liner under the action of the nonuniform loads. The initiation radius has great effect on the slenderness ratio, speed, kinetic energy and shape of tails of the EFP. The appropriate initiation radius was primarily fixed on 20 mm to 30 mm. The experimental result shows a good agreement with results of theoretical analysis and numerical simulations.

Key words: explosion mechanics; explosively formed projectile; three-point initiation; numerical simulation; radius of initiation

CLC number: TJ410.3⁺33; O389

Document code: A

1 Introduction

Germans and Americans first studied the explosively formed projectiles (EFPs). The technology of the EFPs was applied to weapons in the 1960's^[1]. In application systems of the EFPs, the final purpose is to form projectiles that can travel for significant distances before delivering their kinetic energy to the intended target. The crucial technique of the explosively formed projectile is its formation. Among all the factors affecting formation of the EFP, the method of initiation is the most important one. Usually there are four initiation methods such as center point initiation, annular initiation, plane initiation and multi-point initiation. But there is only the multi-point initiation to form the explosively formed projectile with rear fins. The formation of rear fins is an important technology but the mechanism of formation is not quite clear. During the past 10 years, there has been much effort directed at forming stabilizing fins on these penetrators such that they

can "fly" in a stable mode for greater distances. Many foreign researchers^[2-6] have done many experiments and numerical simulations on forming mechanism, movement law and penetrating performance of projectiles with tails and have found several new ways to form the tails. The multi-point initiation is one of ways and it has been one of pivotal technologies of the EFPs. Domestic scholars have also done investigations on it. CAO Bing^[7] analyzed detonation waves interaction and YU Chuan^[8] obtained the projectile with three tails in experiment. But there is few study on formation process and mechanism of tails. Therefore three-dimension numerical simulation was applied in this paper to study the detonation waves interaction, deformation process of the liner, formation process of EFP tails and positions of initiation points influence on tails and so on.

2 Mechanism of three-point initiation

Generally the formation of the EFP lies on the distribution of explosive loads which relies on the structure of detonation wave. So the structure of detonation wave is critical for formation of the EFP.

Received Date: 2005-11-25; **Revised Date:** 2006-05-29

Project Supported: the Premade Study Item of National Defense(413260401)

Biography: LI Cheng-bing (1977 -), male, Ph. D., major in explosion mechanics. e-mail: lichbing@mail.ustc.edu.cn.

If the shaped charge is ignited by the method of center point initiation on side surface, the deformation velocity of liner only depends on the incident angle of detonation wave. According to the detonation wave theory^[9], when the length of charge (L) is less than the maximal curvature radius of the wave front $R_M = (2 - 3.5)D$ (D is the diameter of charge), the curvature radius of wave front (R) equals L , and the wave front is still spherical. Therefore the spherical wave first arrives at the surface of liner. And then elements of the liner with a same radial size are impacted by the same detonation waves at the same time. In other words, they are deformed with a same velocity. Consequently the deformation of liner is axial symmetry and the final EFP is an axial symmetric penetrator. If the shaped charge is initiated by three-point initiation, three detonation waves simultaneously come into being from three initiation points and spread in explosive with same speed. When detonation waves reach their symmetrical planes, they begin to interact, which is shown in Fig. 1(a).

When two detonation waves reach the point A and the separation angle of their wave fronts is zero degree, the normal impact occurs. With the separation angle of the wave front gradually increasing and going beyond zero degree, a series of regularly sloping impacts occur at the symmetrical plane like point B. When the separation angle goes beyond the critical value, Mach impact occurs and Mach wave comes into being^[9]. The formation of Mach wave is shown in Fig. 1(b). With the detonation wave propagating out, a series of Mach waves and three-wave points are formed. There are a lot of regularly sloping impacts and Mach impacts occurring at sides of the normal impact. In area of $O_1O_2O_3$, three detonation waves interact and the center hyper pressure area is formed. Out of the area of $O_1O_2O_3$, detonation waves interact and the peripheral hyper pressure areas around symmetrical planes are produced. Thus the wave front is not spherical wave which consists of single C-J wave after detonation waves interacting. But it is a compound wave consisting of C-J wave and Mach wave. C-J wave and Mach wave alternatively array. There is a discrepancy of the loads intensity and shape of wave front and propagating velocity between Mach wave and C-J wave. Therefore the compound wave front is not as smooth as the spherical wave front^[10].

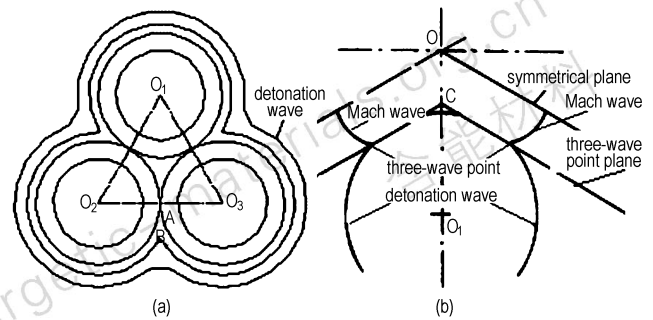


Fig. 1 Sketch of interaction of detonation waves and formation of Mach wave

Since the hyper pressure areas and the normal pressure areas are in a nonuniform arrangement on the plane line to line, the elements of liner with the same radial size are impacted by the nonuniform detonation pressure at the same time. They deform with different velocities. The deformation of the liner with three initiation points differs from that of liner with center initiation point. The projectile with tails is finally made of the liner because of liner elements with different speeds.

3 Numerical simulations of the formation of EFP tails with three initiation points

3.1 Calculating model and relative parameters

The software of LS-DYNA3D was applied to simulate the formation of EFP tails with three initiation points. The calculating model of the EFP device and the layout of initiation points are shown in Fig 2. The device of EFP is simplified to explosive, case, rear cover and liner calculation models. The algorithm of Lagrange hydrocode is adopted in the process of computation. The terminal time of computation is 350 μ s.

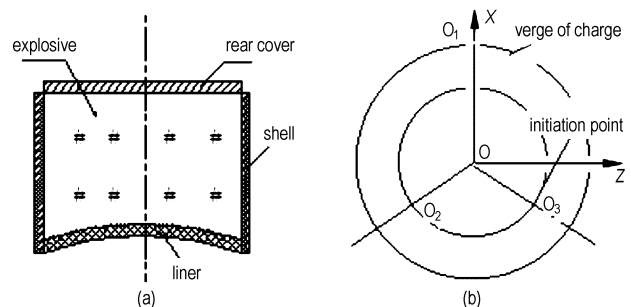


Fig. 2 Sketch of the model and lay out of initiation points

The main charge is B explosive. The material of liner is red copper and the material of case and rear cover is

steel. The values of all parameters are listed in Table 1.

The high-energy explosive material model and JWL equation of state are used for the explosive in calculation. The JWL equation of state is shown that ^[10]:

$$p = A \left[1 - \frac{\omega}{R_1 V} \right] e^{-R_1 V} + B \left[1 - \frac{\omega}{R_2 V} \right] e^{-R_2 V} + \frac{\omega E_0}{V} \quad (1)$$

Where A , B , R_1 , R_2 and ω are input parameters; E_0 is initial specific internal energy; p is C-J pressure; V is relative volume. All the parameters used in calculation are listed in Table 2.

In order to accurately describe the dynamics response of liner material, the material model of the hydro-elastic-plasticity (Steinberg constitutive model) and the Gruneisen state equation are used for the metal liner in calculation. The Steinberg constitutive model is suitable for the plastic strain ratio over 10^5 s^{-1} ^[10]. The Table 3 lists parameters of the state equation and the hydro-elastic-plasticity model of red copper, where σ_s is yield stress; S_1 , S_2 and S_3 are the coefficients of the slope of the $V_s - V_p$ curve; γ is the Gruneisen gamma.

Table 1 Parameters of model

charge diameter D/mm	charge length L/mm	thickness of liner δ/mm	radius of curvature R/mm	thickness of case θ/mm
80	60	4.8	120	4

Table 2 Calculation parameters of explosive

ρ $/\text{g} \cdot \text{cm}^{-3}$	D $/\text{km} \cdot \text{s}^{-1}$	p_{CJ} $/\text{GPa}$	A $/\text{GPa}$	B $/\text{GPa}$	R_1	R_2	ω	E_0 $/\text{kJ} \cdot \text{cm}^{-3}$	V_0
1.710	7.79	28.3	524.3	7.67	4.2	1.1	0.34	8.341	1.0

Table 3 Calculation parameters of copper

ρ $/\text{g} \cdot \text{cm}^{-3}$	σ_s $/\text{GPa}$	C $/\text{km} \cdot \text{s}^{-1}$	S_1	S_2	S_3	γ	a	E_0 $/\text{GPa}$	V_0
8.93	0.09	3.94	1.49	0.6	0	1.99	0.47	0	1.0

The plasticity kinematics hardening model and strain failure mode are utilized for the steel. The failure strain ε is 0.125.

It is necessary to explain the handling method of explosive material in calculation. When the time of calculation is about $60 \mu\text{s}$, the computation grids of the explosive have been badly distorted and time step of calculation sharply falls down. The elements of explosive are deleted. Since the driving action of explosive nearly completes, there is hardly influence on the calculating results.

3.2 Numerical simulation results and discussion

3.2.1 Propagation and interaction of detonation wave in the explosive

The propagating and interacting processes of detonation waves are shown in Fig. 3. When the time is $0.5 \mu\text{s}$ and $2 \mu\text{s}$, the detonation waves propagate outward. When the time is about $2.5 \mu\text{s}$, detonation waves interact. The pressure of three symmetrical planes is obviously higher than that of other areas. With detonation waves propagating in explosive, the interaction goes along the axes of the charge and the hyper pressure areas go along at the same time. The propagating and interacting law of detonation waves accords with the previous analysis.

3.2.2 Detonation loading and the deforming process of liner

Fig. 4 shows the loading processes of detonation and the deforming process of liner. As the time is about $7.5 \mu\text{s}$, the detonation waves reach the surface of liner and the liner starts to be impacted. When the time is $8.0 \mu\text{s}$, the center hyper pressure area is formed on the surface of liner. The metal liner overturns, deforms and shapes, at the same time it expands outward under the action of exploding loads of explosive. When the time is $16.0 \mu\text{s}$ and $20.0 \mu\text{s}$, three pressure marks on the surface of liner are formed by the hyper pressures.

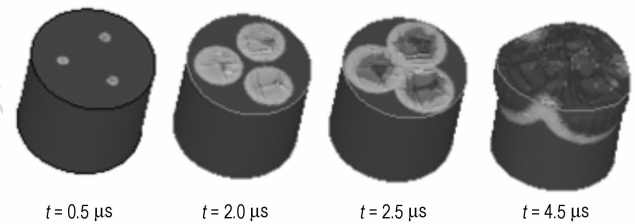


Fig. 3 Propagation and interaction of detonation

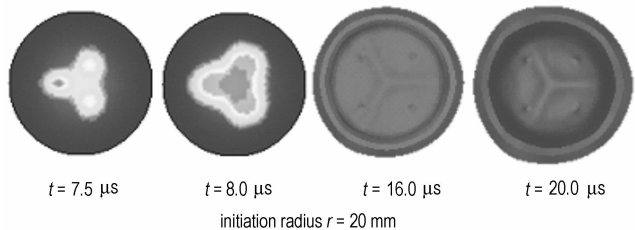


Fig. 4 Detonation loading and the deforming process of liner

3.2.3 Formation of EFP tails

In order to probe into the formation process and mechanism of EFP tails, the point A and the point B on the surface of liner are chosen in Fig. 5. The two-dimen-

sion plane coordinate system of $X-Z$ is established. The origin of coordinate is fixed on the center of liner. The displacement-time Curves of point A and point B on the direction of X axis are shown in Fig. 6. The two curves indicate that the liner first of all expands and then shrinks with the action of exploding loads. Because point A is near to the initiation point and point B is just on the symmetrical plane of detonation waves interacting. That is to say, point B is impacted by the hyper pressure. So the expansion of point B is greater than that of point A .

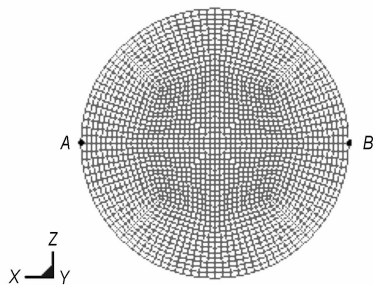


Fig. 5 Point A and B on the surface of liner

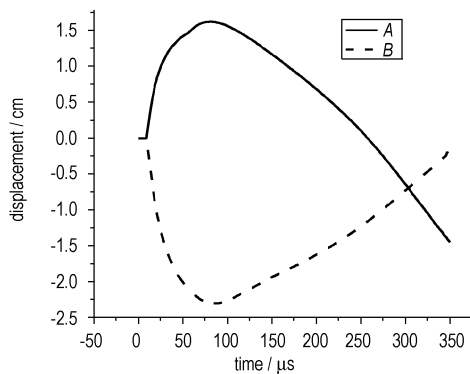


Fig. 6 Displacements of A and B with time

Point B shrinks after expansion and its end displacement is about 2 mm. Namely, the shrinkage of the point B is little on the basis of its initial position. However, point A shrink after expansion and its end displacement maximum is over 15 mm. Therefore, the area of liner near to point B is finally forged to the rear fin of the EFP.

Because the number of initiation point determines

the number of the hyper pressure areas. The formation of the EFP tails lies on the hyper pressure. So the number of the EFP tails depends on the number of initiation points. For example, three hyper pressure areas are formed on the condition of the three-point initiation. Lastly, three rear fins are formed.

3.2.4 Effects of initiation radius on the formation of the EFP with tails

According to the detonation theory, the initiation radius of multi-point initiation has an important influence on the formation of the EFP with tails. Therefore the eight varied values of the initiation radius (r) are chosen to study such as 5, 10, 12.5, 15, 20, 25, 30, 35 mm.

The results of numerical computation are listed in Table 4. With the initiation radius increasing, the head velocity of the EFP increases. When r is 35 mm, the velocity of head is over $1600 \text{ m} \cdot \text{s}^{-1}$. But the tail velocity first increases and then decreases. When r is 20 mm, the tail velocity achieves the maximum. The difference of the head velocity and the tail velocity, the slenderness ratio and kinetic energy of the EFP go ahead with the initiation radius increasing.

Fig. 7 shows the slenderness ratio and shape of the projectiles with varied initiation radius. When r is 35 mm, the shape of the EFP is very slim and it may be torn up. Fig. 8 shows the shape of the EFP tails. When r is 12.5 mm, the tails are primarily formed. When r is 25 mm and 30 mm, the shape of tails is regular.

The penetrating power of the EFP is enhanced as the slenderness ration and kinetic energy increase. But the projectile will be unceasingly lengthened due to the difference of the head velocity and the tail velocity. The projectile may be ripped and its penetrating power may be cut down.

In numerical simulations, when the initiation radius is too small, the velocity, slenderness ratio and kinetic energy of the EFP are also small. Moreover the EFP tails are

Table 4 Effects of initiation radius on the parameters of EFP

initiation radius/mm	$r = 5.0$	$r = 10.0$	$r = 12.5$	$r = 15.0$	$r = 20.0$	$r = 25.0$	$r = 30.0$	$r = 35.0$
velocity of head/ $\text{m} \cdot \text{s}^{-1}$	1435	1435	1469	1493	1521	1545	1583	1623
velocity of tail/ $\text{m} \cdot \text{s}^{-1}$	1421	1421	1438	1447	1470	1438	1422	1379
difference/ $\text{m} \cdot \text{s}^{-1}$	14	14	31	46	101	107	161	244
slenderness ratio	2.52	2.56	4.0	5.25	5.53	6.87	7.10	8.12
kinetic energy/ 10^5 J	2.435	2.523	2.568	2.597	2.696	2.756	2.816	2.937

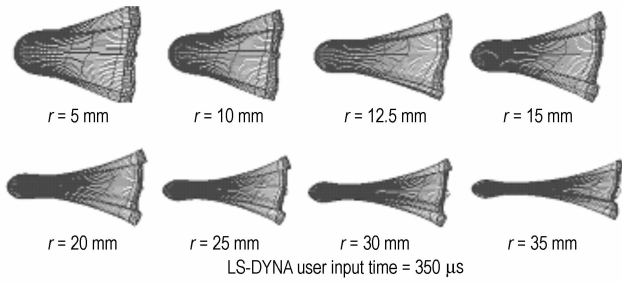


Fig. 7 Shape of the EFP projectiles

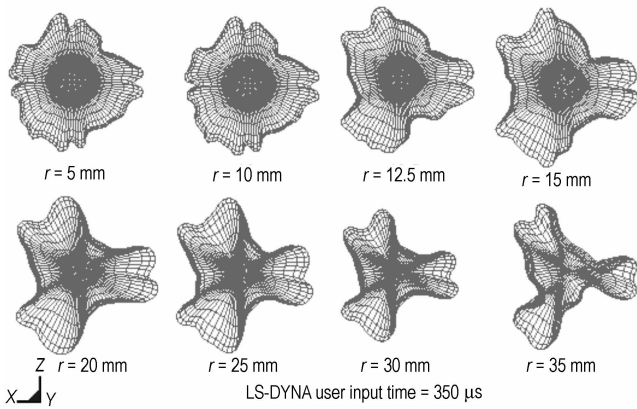


Fig. 8 Tails of EFP with varied initiation radius

not formed. But the EFP may be easily broken with high gradient of velocity when the initiation radius is too big. The appropriate initiation radius is primarily fixed on 20 mm to 30 mm according to the simulating results.

4 Experimental

Three $\varnothing 80$ mm EFP warheads were made in the experiment. The first warhead was initiated with center point and other warheads were ignited with three-point. The initiation radius was fixed on 25 mm and 28 mm individually according to results of simulations. The other parameters were same with these of simulation model. Two copper foil speed targets were used to record velocities of EFP and their interval was 1 m. Four net targets were utilized to record flying stability and were positioned in the distance of 10 m, 20 m, 30 m and 40 m. The after effect target which was a 50 mm steel plate was fixed in distance of 40 m (500D). All impact positions on net targets were processed on the coordinate plane. Results are listed in Table. 5.

Table 5 EFP experimental results

number	velocity/ $m \cdot s^{-1}$			coordinates of impact on net targets/cm				after effect target
	speed target I	speed target II	speed drop / $m \cdot s^{-1}$	target I	target II	target III	target IV	
1(0 mm)	1329.6	1318.5	11.1	(0, +2)	(-8, +13)	(-17, +24)	(-25, +34)	embedding
2(25 mm)	1517.3	1513.8	3.5	(+2, +1)	(+2, +5)	(+7, +10)	(+13, +10)	32 mm × 30 mm
3(28 mm)	1536.8	1533.1	3.7	(0, +2)	(-1, +3)	(-9, +6)	(-17, +13)	33 mm × 31 mm

Experimental results present that velocity of projectile with three-point initiation is higher and speed drop is lower. Coordinates of impact indicate the projectile which is formed by three-point initiation can fly in a better mode. Moreover, its penetration ability is stronger and it can break through the 50 mm after effect target. The initiation radius of 25 mm and 28 mm have a nearly same influence on velocity, speed drop, flying stability and penetration ability of projectile.

These results just validate anterior investigations. Compared with center point initiation, detonation waves impact each other to form hyper pressure areas and the liner is deformed by stronger explosively loads under condition of three-point initiation. At the same time, hyper pressure on symmetrical planes make liner to be forged a projectile with three tails. Tails can effectively cut down

its speed drop and keep its good aerodynamic stability in the great distances. It is complicated that initiation parameters affect performance of EFP. Much effort should be directed to probe into it.

5 Conclusions

(1) Detonation waves impact each other to form hyper pressure areas under condition of three-point initiation. The liner is deformed by strong explosively loads and three pressure marks on the surface of liner are formed.

(2) Results of theoretical analysis and simulations show the liner overturns and deforms under the action of the nonuniform loads of explosive. Formation of EFP tails is attributed to the different displacements of the liner elements under the action of the nonuniform exploding loads. The initiation radius has great effect on the slen-

